

Effect of Nucleating Agent Addition on Crystallization of Isotactic Polypropylene

Y. FENG,* X. JIN, J. N. HAY

School of Metallurgy & Materials, University of Birmingham, Edgbaston, Birmingham B15 2TT, United Kingdom

Received 13 August 1997; accepted 30 December 1997

ABSTRACT: The isothermal and nonisothermal crystallization kinetics of nonnucleated and nucleated isotactic polypropylene (iPP) were investigated by DSC and a polarized light microscope with a hot stage. Dibenzylidene sorbitol (DBS) was used as a nucleating agent. It was found that the crystallization rate increased with the addition of DBS. The influence of DBS on fold surface energy, σ_e , was examined by the Hoffman and Lauritzen nucleation theory. It showed that σ_e decreased with the addition of DBS, suggesting that DBS is an effective nucleating agent for iPP. Ozawa's theory was used to study the nonisothermal crystallization. It was found that the crystallization temperature for the nucleated iPP was higher than that for nonnucleated iPP. The addition of DBS reduced the Ozawa exponent, suggesting a change in spherulite morphology. The cooling crystallization function has a negative exponent on the crystallization temperature. © 1998 John Wiley & Sons, Inc. *J Appl Polym Sci* 69: 2089–2095, 1998

Key words: nucleating agent; isothermal crystallization; nonisothermal crystallization; isotactic polypropylene

INTRODUCTION

It is known that isotactic polypropylene (iPP) shows unsatisfactory impact strength at low temperatures because of its production of large spherulites when it crystallizes from the melt. Three means are often used to overcome this shortcoming. The first is the production of physical blends of the homopolymer with various types and amounts of rubber,^{1,2} the second is developing the copolymer,³ and the third is adding nucleating agents to lower the dimensions of the spherulite.^{4,5}

Nucleating agents are used routinely in industrial practice to shorten injection-molding cycles and/or to improve optical and mechanical proper-

ties to crystallize the polymer by reducing the spherulite size. Various authors have conducted fundamental studies regarding the influence of nucleating agents on the kinetics of polymer crystallization from the melt.^{6–8} However, the effectiveness of a nucleating agent varies from polymer to polymer. Much work has been done on the effects of nucleating agents on isothermal crystallization of iPP.^{4–8} However, the actual processing is performed under nonisothermal conditions. So nonisothermal experiments are often a useful complement to understand crystallization behavior of a semicrystalline polymer in its processing. The objective of this study was to analyze the effect of a nucleating agent, dibenzylidene sorbitol (DBS), on the isothermal and nonisothermal crystallization of iPP. Knowledge of the effects of such a nucleating agent on isothermal and nonisothermal crystallization is useful in determining processing conditions and in evaluating the effectiveness of this nucleating agent.

Correspondence to: Y. Feng.

* Present address: Department of Chemistry, University of Waterloo, Waterloo, Ontario N2L 3G1, Canada.

Journal of Applied Polymer Science, Vol. 69, 2089–2095 (1998)

© 1998 John Wiley & Sons, Inc.

CCC 0021-8995/98/102089-07

EXPERIMENTAL

Materials

Commercially available iPP (grade HV206, supplied by Solvay) was used in this study. DBS (supplied by Milliken Chemical, Millad 3905) was a white powder with a size of $<250 \mu\text{m}$. The melting point for DBS is 220°C , and the crystallization temperature is 180°C .

Specimen Preparation

DBS was added to the iPP by mixing the polymer and DBS on a heated two roll mill at 190°C .

Apparatus and Experimental Procedures

A Perkin–Elmer differential scanning calorimeter (DSC-2), interfaced with a BBC-Master computer via an analogue to digital converter was used. The temperature scale of the DSC was calibrated from the melting points (mp) of zone refined stearic acid (mp, 343.50 K) and high purified metals such as indium (mp, 429.78 K), tin (mp, 505.05 K), lead (mp, 600.50 K), and zinc (mp, 692.65 K). A 10-mg sample containing DBS (in an aluminum pan) was heated above 470 K in N_2 , kept 5 min at that temperature, and then cooled to crystallizing temperature (T_c) rapidly to observe the process of crystallization.

The spherulite growth was investigated by a polarized light microscope (Leitz Dialux) with a Linkam hot stage (TH600) and a temperature controller (PR600), working in the range of ambient temperature to 773 K with heating rates of $0.1\text{--}99 \text{ K min}^{-1}$. Calibration of the hot stage was achieved by an electronic method with a standard resistance across the output from the temperature controller. A very small amount of sample (a few milligrams) was sandwiched between two circular acetone cleaned glass plates of about 0.5-cm diameter. The hot stage was then heated to above the melting point of iPP. After 5 min at the melting temperature, the hot stage was set to the crystallization temperature and reached this temperature in approximately 30 s. Spherulite growth was recorded at the crystallization temperature as a function of time using visual tape.

RESULTS AND DISCUSSION

Isothermal Crystallization

Overall Crystallization Kinetics

The Avrami equation has been widely used to analyze isothermal crystallization⁹:

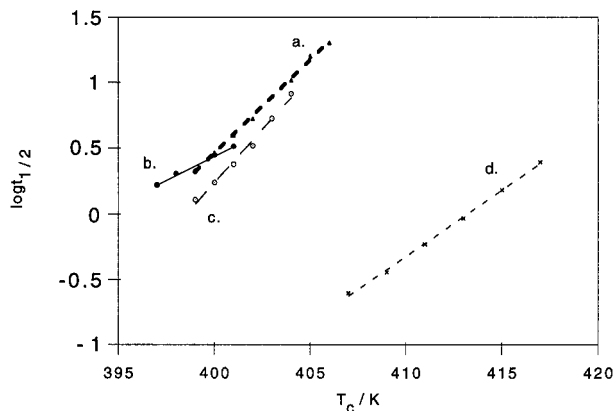


Figure 1 Variation of crystallization half-life with temperature: (a) iPP, (b) 0.25% DBS, (c) 0.5% DBS, and (d) 1% DBS.

$$X_c(t)/X_c(0) = 1 - \exp(-kt^n) \quad (1)$$

where $X_c(t)$ and $X_c(0)$ are the crystallinity at time t and the crystallinity at the end of crystallization, respectively. The time t was measured from the time when samples were cooled to the crystallization temperature. Because determination of the absolute degree of crystallization is not required in the Avrami analysis, the ratio of the area at time t and the area of the whole exotherm was used for $X_c(t)/X_c(0)$. The exponent n is dependent on the type of nucleation and the crystal growth geometry; the parameter k is also a function of nucleation and growth. The Avrami parameters n and k are determined by taking the double logarithm of eq. (1) to yield a plot of $\ln\{-\ln[1 - X_c(t)/X_c(0)]\}$ versus $\ln t$, and k can also be obtained from the expression

$$k = \frac{\ln 2}{t_{1/2}^n} \quad (2)$$

where the half-life, $t_{1/2}$, is the time taken for 50% of the total crystallization to occur.

Crystallization rates of polymers can be expressed in terms of $t_{1/2}$ obtained from the isothermal exotherms of the DSC results. The shorter the half-life, the faster the crystallization rate, and vice versa. Figure 1 gives the results of the relationship between $t_{1/2}$ and crystallization temperature, T_c , for nonnucleated and nucleated samples. Figure 1 indicates that the crystallization rate increases with decreasing T_c . When the T_c is lowered, the driving force (which is proportional to the difference between the equilibrium melting point and the crystallization tempera-

Table I Values of Crystallographic Unit Cell Dimension for Polypropylene

(110) Growth Plane	
a_0 (m):	5.49×10^{-10}
b_0 (m):	6.26×10^{-10}
$a_0 b_0$ (m ²):	3.43×10^{-19}

ture) for crystallization increases because of the increased nucleation density and growth rate of the spherulites. The experimentally accessible crystallization temperatures for the nucleated samples also shown in Figure 1 were higher than those accessible for the nonnucleated samples, indicating that the addition of DBS increased crystallization; furthermore, the crystallization rate increased with increasing the amount of DBS because of the increase of nucleation density. Similar results were obtained for sorbitol derivatives by Kim et al.¹⁰ who found that the number of effective nuclei in the nucleated samples was estimated to be 3×10^2 – 10^5 times larger than that in the neat iPP.

The Hoffman and Lauritzen nucleation theory has been used to quantify polymer crystallization kinetics in the melt.^{11,12} The growth rate of polymers during crystallization can be described within a given regime by the equations

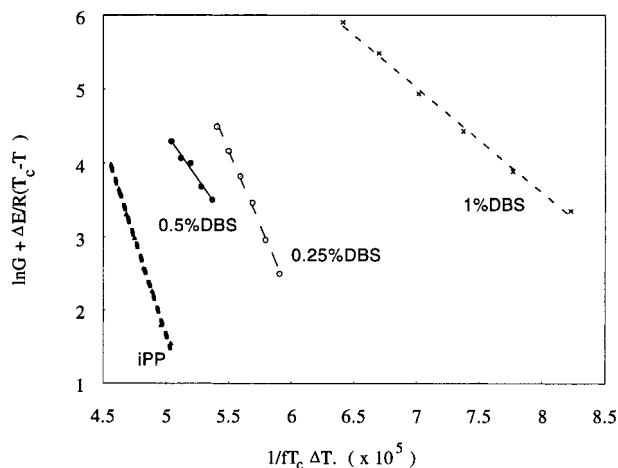
$$G = G_0 \exp \left[-\frac{\Delta E}{R(T_c - T_\infty)} \right] \exp \left[-\frac{K_g}{T_c \Delta T} \right] \quad (3)$$

$$\ln G + \frac{\Delta E}{R(T_c - T_\infty)} = \ln G_0 - \frac{K_g}{T_c \Delta T} \quad (4)$$

where

$$K_g = \frac{4b\sigma\sigma_e T_m^0}{\Delta H_m k} \quad (5)$$

Here G_0 is the preexponential factor containing quantities not strongly dependent on the temperature; ΔE is a “universal” constant characteristic of the activation energy of chain motion (reptation) in the melt, $\Delta E = 6280 \text{ J mol}^{-1}$; R is the gas constant; T_∞ is the theoretical temperature at which all motion associated with viscous flow or reptation ceases and is defined as $T_\infty = T_g - 30 \text{ K} = 239.6 \text{ K}$; b is the monolayer thickness; σ is the lateral surface energy; σ_e is the fold surface energy; k is the Boltzman constant; T_c is the crystallization temperature; T_m^0 is the equilibrium

**Figure 2** Relationship between $\ln G + \Delta E/R(T_c - T)$ and $1/fT_c \Delta T$ for samples crystallized at various T_c temperatures.

melting temperature; ΔT is the supercooling and is equal to $T_m^0 - T_c$; and ΔH_m is the heat of fusion.

Equations (3)–(5) are used for crystallization occurring in regimes I and III. The slope of a plot of $\ln G + \Delta E/R(T_c - T_\infty)$ with $1/T_c \Delta T$ yields the fold surface energies. In determining the σ_e , the σ is estimated using the following equation:

$$\sigma = \alpha(a_0 b_0)^{1/2} \Delta H_m \quad (6)$$

where α was derived empirically to be 0.1 and is patterned after the Thomas–Stavely relationship,¹³ and we take $1/t_{1/2}$ as G . The material constants for iPP used in the analysis are listed in Table I. The material constants for nucleated iPP used in the analysis are the same as those listed in Table I. The equilibrium melting points were determined by DSC via the Hoffman–Weeks method.¹⁴

The K_g values from Figure 2 were obtained from the slope (Table II). The values of σ_e for the nonnucleated and nucleated samples listed in Table II were derived from K_g using eqs. (3)–(5). According to Beck’s criteria, a good nucleating

Table II Kinetic Parameters for Nonnucleated and Nucleated iPP from DSC

Sample	$K_g (\times 10^{-5})/K^2$	$\sigma_e (\text{J m}^{-2})$
iPP	5.2268	0.1068
iPP + 0.25% DBS	4.0182	0.0821
iPP + 0.5% DBS	2.4307	0.0497
iPP + 1% DBS	1.4185	0.0290

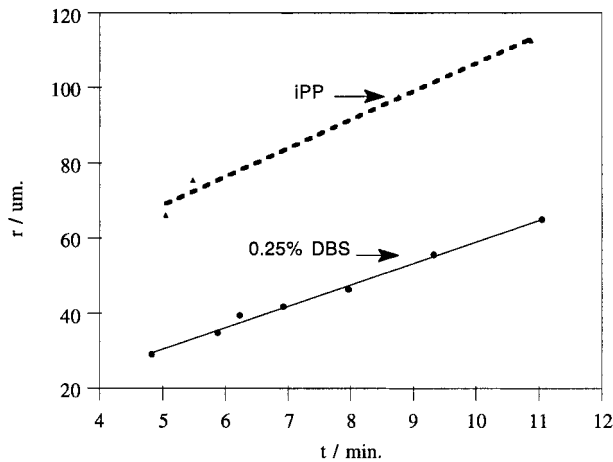


Figure 3 Effect of DBS on spherulite growth of iPP.

agent reduces the interfacial surface free energy.¹⁵ In Table II shows that the addition of nucleating agent reduced the σ_e . The lowering of σ_e with the addition of DBS can be due to the occurrence of multiple nucleation, leading to the formation of loops and tie molecules, and dangling chain ends from primary and secondary crystallization. These results indicated that DBS is an effective nucleating agent for iPP. Smith et al.¹⁶ studied the mechanism of action of DBS as a nucleating agent for iPP. They proposed that DBS can stabilize the helical form of PP at the molecular level. Through molecular modeling, they demonstrated that the nucleating ability can be correlated with van der Waals attractions of the individual nucleator molecules with the helical form of PP.

Spherulite Radical Growth Rate

Growth rate studies for nucleated polymers are experimentally difficult to obtain because of the reduced spherulite size. In this work, polarized light microscopy (PLM) observations were carried out only for iPP and iPP containing 0.25% DBS, because for samples containing 0.5 and 1% DBS the spherulites filled the volume rather quickly and spherulitic growth could not be monitored visually.

The measured spherulite radius was plotted against time. A representative plot of spherulite radius versus time is given in Figure 3. It was obvious that the size of the spherulite was largely reduced by the addition of DBS. The growth rate was taken as the slope of the linear portion of

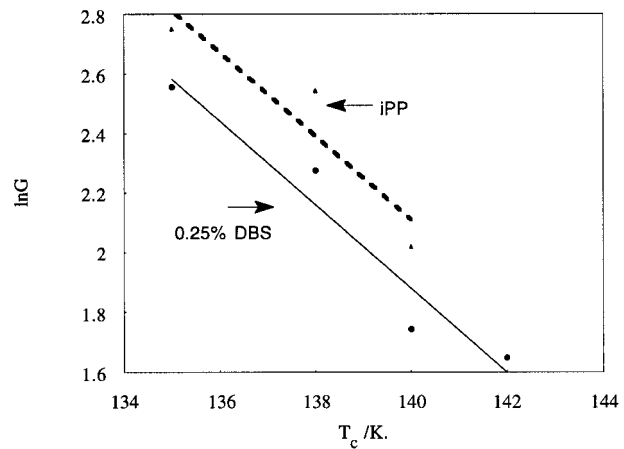


Figure 4 Effect of DBS on growth rate for isothermal crystallization of iPP.

the plot. Figure 4 shows the effect of DBS on the relationship between $\ln G$ and T_c . It can be seen that DBS has little influence on the growth rate of the spherulite. As analyzed above, we can see from Figure 5 and Table III that in using PLM we also obtained the reduction of σ_e .

Nonisothermal Crystallization

Several models have been proposed for the theoretical treatment of isothermal crystallization kinetics.¹⁷⁻¹⁹ Conversely, only a few models have been developed to explain nonisothermal crystallization, the most important ones being those of Jeziorny,²⁰ Ziabicki,²¹ and Ozawa.²² In the present work, Ozawa's theory is adopted to describe

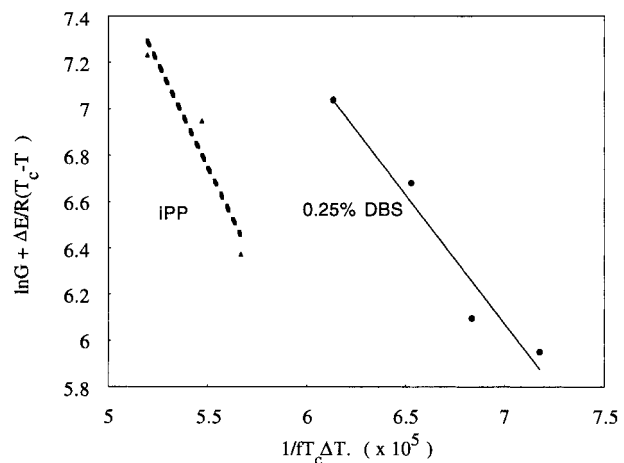


Figure 5 Effect of DBS on Hoffman-Lauritzen growth rate.

Table III Kinetic Parameters for Nonnucleated and Nucleated iPP from PLM

Sample	$K_g (\times 10^{-5})/K^2$	$\sigma_e (\text{J m}^{-2})$
iPP	1.7787	0.0364
iPP + 0.25% DBS	1.1135	0.0228

the effect of the nucleating agent DBS on the crystallization of i-PP at a constant cooling rate.

The theoretical development by Ozawa²² is based on constant cooling conditions and is an extension of the mathematical derivation by Evans.¹⁸ Crystals originate from nuclei and expand as spherulites, and the radial growth rate is constant at a given temperature. The untransformed volume fraction $1 - X(T)$ at temperature T is related to the cooling rate R by the expression

$$\ln\{-\ln[1 - X(T)]\} = X_c - n \ln R \quad (7)$$

where X_c is a constant and n indicates the type of nucleation and morphology. The constant n at a specific temperature is obtained from the slope of the plot of $\ln\{-\ln[1 - X(T)]\}$ versus $\ln R$; X_c is obtained from the intercept of the same plot. In polymers where secondary crystallization occurs, the Ozawa method cannot be applied.²³ Isothermal crystallization studies²⁴ have shown that secondary crystallization does not play an important role in iPP crystallization. Ozawa suggested that plots of $\ln\{-\ln[1 - X(T)]\}$ versus temperature at different cooling rates can be superimposed by longitudinal shifts of length $n \ln R$ if there is no appreciable secondary crystallization.

Figure 6 shows the crystallization curves obtained for different cooling rates. As in other studies on crystallization of iPP,^{25,26} it was also found for nucleated iPP that the crystallization temperature decreased with the increase of cooling rate. With an increasing amount of nucleating agent, the crystallization temperature increased (Fig. 7).

The Ozawa analysis has been used to study the dependence of morphology on temperature during nonisothermal crystallization.^{22,23} There are two previous studies on iPP^{25,26} that showed that iPP can be analyzed by the Ozawa analysis. However, there is no literature on applying the Ozawa analysis to a nucleated polymer.

For each cooling rate R , the untransformed volume fraction $1 - X(T)$ at a given temperature T can be determined from the experimental curves

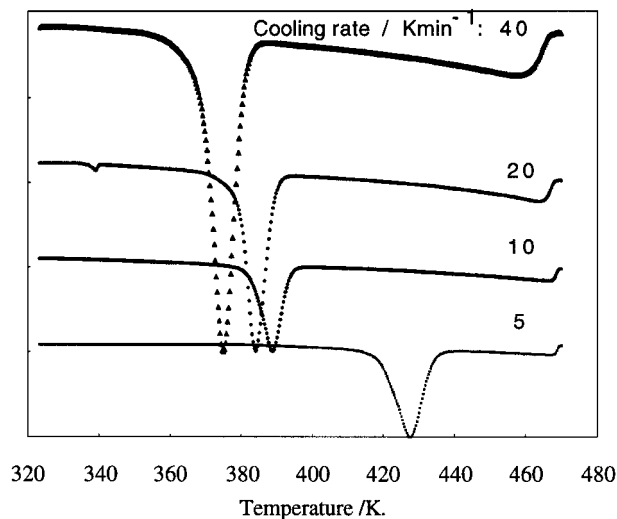


Figure 6 DSC curves corresponding to the crystallization of iPP containing 0.25% DBS at different cooling rates.

of Figure 6, as suggested by eq. (7). Then $\ln\{-\ln[1 - X(T)]\}$ is plotted as a function of $\ln R$ (Fig. 8). If eq. (7) is valid, the curve corresponding to a given temperature must be a straight line whose slope is the Ozawa exponent n and whose intercept is the cooling crystallization function X_c . Figure 8 shows the good agreement between the experimental results and theoretical prediction.

In nonnucleated iPP the n increased as the crystallization temperature was lowered. This trend of n with crystallization temperature agrees with the finding of Monasse and Haudin.²⁶ The range of n obtained in this study indicated truncated 3-dimensional spherulites resulting from instantaneous nucleation. As the crystallization

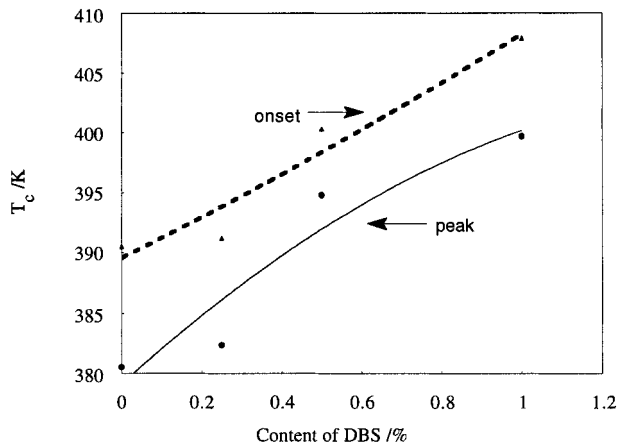


Figure 7 Effect of DBS on the crystallization temperature.

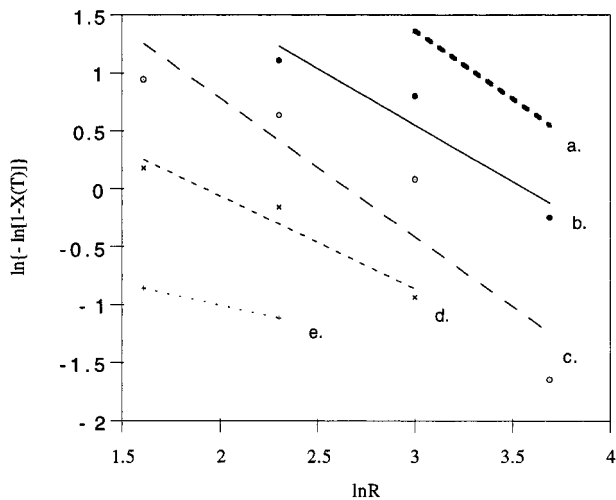


Figure 8 Interpretation of the DSC curves using Ozawa's theory for iPP sample containing 1% DBS. T_c : (a) 385 K, (b) 390 K, (c) 395 K, (d) 400 K, and (e) 405 K.

temperature was lowered, the nucleation changed from instantaneous to sporadic, causing n to increase (Fig. 9).

The n versus temperature plots for the nucleated mixtures (Fig. 9) showed considerably more scatter than nonnucleated iPP. However, the trend was evident that n decreased as the temperature was increased. Again the values indicated truncated 3-dimensional spherulites.

The cooling crystallization function, determined from the intercept of the double logarithm plot of eq. (7), is shown in Figure 10 as a function of crystallization temperature. Figure 10 indicates that the cooling crystallization function has

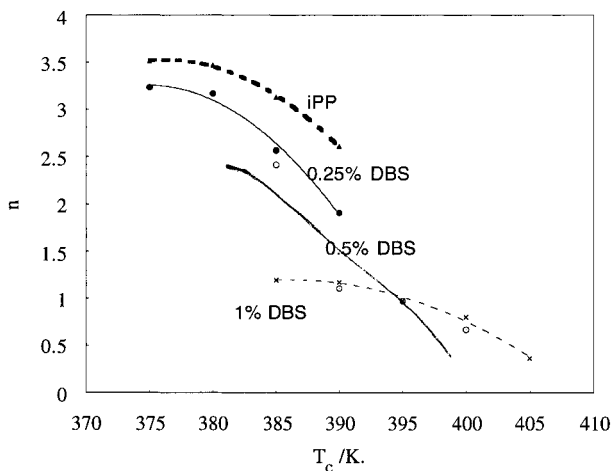


Figure 9 Plot of Ozawa exponent versus T_c for nonnucleated and nucleated iPP.

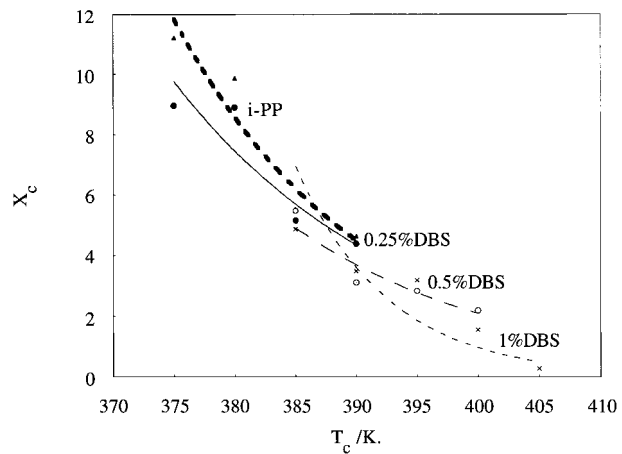


Figure 10 Effect of DBS and T_c on the cooling crystallization function.

a negative exponential dependence on temperature.

CONCLUSION

We can see from the above analysis that the crystallization temperatures for the nucleated samples were higher than those for nonnucleated samples. The crystallization rate increased with the addition of DBS and with the increasing amount of DBS. The fold surface energy was calculated by Hoffman and Lauritzen theory.^{11,12} It showed that the addition of DBS can reduce the fold surface energy, indicating that DBS is an effective nucleating agent.

The Ozawa theory can be used to study the nonisothermal crystallization of nucleated iPP.²² The Ozawa exponents indicated that the mechanism for crystallization of iPP was usually instantaneous nucleation with truncated 3-dimensional spherulites. At a lower crystallization temperature, sporadic nucleation occurred. The addition of DBS reduced the value of the Ozawa exponent, suggesting a change in spherulitic morphology. The cooling crystallization function has a negative exponential dependence on T_c . It is suggested that increased truncation due to faster impingement must occur before 3-dimensional growth can occur.

REFERENCES

1. B. Z. Jang, D. R. Uhlman, and J. B. Vander Sande, *Polym. Eng. Sci.*, **25**, 643 (1985).

2. B. Z. Jang, D. R. Uhlman, and J. B. Vander Sande, *J. Appl. Polym. Sci.*, **29**, 3409 (1984).
3. K. Hayashi, T. Morioka, and S. Toki, *J. Appl. Polym. Sci.*, **48**, 411 (1993).
4. F. J. Rybuikar, *J. Appl. Polym. Sci.*, **13**, 827 (1969).
5. F. L. Binsbergen and B. G. M. Delarge, *Polymer*, **11**, 309 (1970).
6. H. N. Beck and H. D. Ledbetter, *J. Appl. Polym. Sci.*, **9**, 2131 (1965).
7. H. N. Beck, *J. Polym. Sci. Phys.*, **4**, 631 (1966).
8. Yu. K. Godovsky and G. L. Slonimsky, *J. Polym. Sci. Phys.*, **12**, 1053 (1974).
9. (a) M. Avrami, *J. Chem. Phys.*, **7**, 1103 (1939); (b) M. Avrami, *J. Chem. Phys.*, **8**, 212 (1940); (c) M. Avrami, *J. Chem. Phys.*, **9**, 177 (1941).
10. C. Y. Kim, Y. C. Kim, and S. C. Kim, *Polym. Eng. Sci.*, **33**, 1445 (1993).
11. J. D. Hoffman and J. I. Lauritzen, *J. Chem. Phys.*, **31**, 1680 (1959).
12. J. I. Lauritzen and J. D. Hoffman, *J. Appl. Phys.*, **44**, 4340 (1973).
13. D. G. Thomas and L. A. K. Stavely, *J. Chem. Soc.*, **1952**, 4569 (1952).
14. J. D. Hoffman and J. J. Weeks, *J. Chem. Phys.*, **37**, 1723 (1962).
15. H. N. Beck, *J. Appl. Polym. Sci.*, **19**, 371 (1975).
16. T. L. Smith, D. Masilamani, L. K. Bui, Y. P. Khanna, R. G. Bray, W. B. Hammand, S. Curran, J. J. Belles, and S. B. Castelli, *Macromolecules*, **27**, 3147 (1994).
17. E. J. Clark and J. D. Hoffman, *Macromolecules*, **17**, 878 (1984).
18. U. R. Evans, *Trans. Faraday Soc.*, **41**, 369 (1945).
19. M. C. Tobin, *J. Polym. Sci. Phys.*, **15**, 2269 (1977).
20. A. Jeziorny, *Polymer*, **19**, 1142 (1978).
21. A. Ziabicki, *Appl. Polym. Symp.*, **6**, 1 (1967).
22. T. Ozawa, *Polymer*, **12**, 150 (1971).
23. M. Eder and A. Wlochowicz, *Polymer*, **24**, 1593 (1983).
24. M. Gordon and J. H. Hillier, *Polymer*, **6**, 213 (1965).
25. A. Wlochowicz and M. Eder, *Colloid Polym. Sci.*, **261**, 621 (1983).
26. B. Monasse and J. M. Haudin, *Colloid Polym. Sci.*, **264**, 117 (1986).